catalase isolated from *Lactobacillus plantarum* and in a recently characterized ribonucleotide reductase from *Brevibacterium ammoniagenes*.[4c]

Oxidation reactions of species containing LMn^{III} or $L'Mn^{III}$ units in alkaline aqueous solution in the presence of oxygen afford the tetranuclear $[L_4Mn_4(\mu\text{-}O)_6]^{4+}$ and the dimeric $[L'_2Mn_2(\mu\text{-}O)_3]^{2+}$ cations, respectively, which contain manganese(IV) centers. In the latter complex the unprecedented short $Mn^{IV}\cdots Mn^{IV}$ distance and its magnetic properties may indicate the presence of a bonding interaction between the two manganese(IV) centers, but the data at hand do not allow an unambiguous assignment. This compound represents a fascinating borderline case.

Acknowledgment. This work was supported by the Deutsche Forschungsgemeinschaft and the Fonds der Chemischen Industrie. We thank Drs. A. Neves, K. Pohl and E. Wasielewska for their help with the cyclic voltammetric measurements.

Supplementary Material Available: Lists of bond distances, bond angles, and anisotropic displacement parameters and calculated positional parameters for hydrogen atoms (Tables S2-14) of complexes **4**, **7**, **8**, and **9**, positional and isotropic thermal parameters of the BPh_4 anion in **4** (Table S1), and magnetic susceptibility data for **8** (Table S14) (22 pages). Ordering information is given on any current masthead page.

The Dynamics of Reaction of a Water-Soluble and Non-μ-Oxo Dimer Forming Iron(III) Porphyrin with *tert*-Butyl Hydroperoxide in Aqueous Solution. 1. Studies Using a Trap for Immediate Oxidation Products

John R. Lindsay Smith,† P. N. Balasubramanian, and Thomas C. Bruice*

Contribution from the Department of Chemistry, University of California at Santa Barbara, Santa Barbara, California 93106. *Received March 28, 1988*

Abstract: A kinetic and product study has been carried out in aqueous solution for the reaction of *t*-BuOOH with the water-soluble and non-μ-oxo dimer forming (5,10,15,20-tetrakis(2,6-dimethyl-3-sulfonatophenyl)porphinato)iron(III) hydrate ((**1**)$Fe^{III}(X)$; where X = H_2O or HO^-). Reactions were studied at 30 °C and μ = 0.22 (with $NaNO_3$) between pH 2.22 and 12.96, and the course of reaction was followed by employing the water-soluble 2,2'-azinobis(3-ethylbenzthiazoline-6-sulfonate) (ABTS) as a trap for oxidant intermediates. One-electron oxidation of ABTS provides the chromophoric radical cation $ABTS^{\cdot+}$ (λ_{max} 660 nm). Reactions were carried out under the pseudo-first-order conditions of [ABTS] $\gg$ [*t*-BuOOH] $\gg$ [(**1**)$Fe^{III}(X)$] using between 10- and 100-turnovers of the iron(III) porphyrin catalyst. The reaction is first order in both $[t\text{-BuOOH}]_i$ and $[(\mathbf{1})Fe^{III}(X)]_i$, and both initial and first-order rate constants are independent of $[ABTS]_i$, ionic strength, and buffer concentrations (buffers employed and pH values for buffer dilution experiments: $ClCH_2COOH/ClCH_2COO^-$ (pH 3.45), CH_3COOH/CH_3COO^- (pH 4.60), $H_2PO_4^-/HPO_4^{2-}$ (pH 6.87), $H_3BO_3/H_2BO_3^-$ (pH 8.66), and HCO_3^-/CO_3^{2-} (pH 9.13), collidine/collidine·H^+ (6.18, 6.98, 8.15)). It follows that the rate-determining step occurs after ligation of available alkyl hydroperoxide species (*t*-BuOOH and *t*-$BuOO^-$, pK_a = 12.8) with iron(III) porphyrin species ((**1**)$Fe^{III}(H_2O)_2$ and (**1**)$Fe^{III}(H_2O)(OH)$, pK_a = 7.2), and that these reactions are not subject to either general-acid nor general-base catalysis. A plot of the log of the pH dependent second-order rate constant ($k_{obsd}/[(\mathbf{1})Fe^{III}(X)]$) vs pH may be fit by an equation (eq 3) containing the sum of four terms (*A*, *B*, *C*, *D*). The equation contains four apparent acid dissociation constants. There are, however, only two acid dissociation constants associated with the reactants. The pH dependence of the reaction may be explained by taking into account the acid dissociations of *t*-BuOOH when ligated to both (**1**)$Fe^{III}(H_2O)$ and (**1**)$Fe^{III}(OH)$. With $Ph(CH_3)_2C\text{–}OOH$ as the hydroperoxide the products are $Ph(CH_3)C{=}O$ and CH_3OH. The product $Ph(CH_3)C{=}O$ establishes the formation of $Ph(CH_3)_2C\text{–}O^{\cdot}$ from alkyl hydroperoxide. With *t*-BuOOH the products are $(CH_3)_2C{=}O$ and CH_3OH. When ABTS is used as a trap for intermediate oxidants, the yield of $ABTS^{\cdot+}$ is virtually constant (70%) between pH 4 and 10, assuming two ABTS molecules undergo $1e^-$ oxidation for each *tert*-butyl hydroperoxide moiety reacted. With ABTS the products of *tert*-butyl hydroperoxide decomposition are *t*-BuOH, $(CH_3)_2CO$, and CH_3OH. In the absence of the ABTS trap $(CH_3)_2CO$ (90%) is the predominant product. Increasing concentrations of ABTS result in the yield of $(CH_3)_2CO$ decreasing asymptotically to 15% and the yield of *t*-BuOH increasing to 84%. The following alternate mechanistic proposals have been advanced: (i) The immediate product is the solvent caged species [(**1**)$Fe^{IV}(X)(OH)$-*t*-$BuO^{\cdot}$] and ~15% of the *t*-$BuO^{\cdot}$ fragments within the solvent cage to provide $(CH_3)_2CO$ and $CH_3^{\cdot}$. The *t*-$BuO^{\cdot}$ which escapes the solvent cage either undergoes the same reaction or is trapped by ABTS depending upon the latter's concentration. Formation of CH_3OH would occur via reaction of $CH_3^{\cdot}$ with (**1**)$Fe^{IV}(X)(OH)$ much as in the rebound mechanism for hydrocarbon hydroxylation. (ii) In competitive mechanisms 15% of *t*-BuOOH is consumed to provide the caged species [(**1**)$Fe^{IV}(X)(OH)$-*t*-$BuO^{\cdot}$] accompanied by fragmentation of $(CH_3)_3CO^{\cdot}$ within the solvent cage etc. The competing reaction would then involve the reduction of the iron(III) porphyrin by the hydroperoxide to form the species (**1**)$Fe^{II}(X)$ + *t*-$BuOO^{\cdot}$ followed by the rapid conversions 2 *t*-$BuOO^{\cdot} \rightarrow$ 2 *t*-$BuO^{\cdot}$ + O_2 and O_2 + 2 (**1**)$Fe^{II}(X) \rightarrow \rightarrow$ 2 (**1**)$Fe^{IV}(O)(X)$.

In previous studies the reaction of hydrogen peroxide with (5,10,15,20-tetrakis(2,6-dimethyl-3-sulfonatophenyl)porphinato)iron(III) and -manganese(III) hydrates ((**1**)$Fe^{III}(X)$ and (**1**)$Mn^{III}(X)$, respectively (where X = H_2O or HO^-)) were investigated in water as a function of pH and buffer acid and base concentrations.[1,2] The pH-dependent second-order rate constants

† Department of Chemistry, University of York, York, England.

(1) Zipplies, M. F.; Lee, W. A.; Bruice, T. C. *J. Am. Chem. Soc.* **1986**, *108*, 4433.

(2) Balasubramanian, P. N.; Schmidt, E. S.; Bruice, T. C. *J. Am. Chem. Soc.* **1987**, *109*, 7865.

0002-7863/88/1510-7411$01.50/0

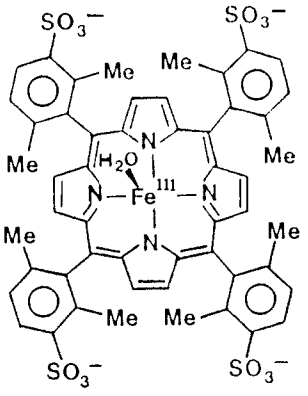

(k_{ly}) for the reaction of hydrogen peroxide with both (**1**)Fe^{III}(X) and (**1**)Mn^{III}(X) were found to be independent of the concentrations of buffer oxyanion bases and their conjugate acids across the pH range investigated. Imidazole was found to form a 1:1 complex with (**1**)$Mn^{III}(H_2O)_2$ with a resultant increase in the second-order rate constant for reaction with hydrogen peroxide of 10-fold. Neither imidazole or 2,4,6-trimethylpyridine nor their conjugate acids are general catalysts for the reaction of hydrogen peroxide with (**1**)Mn^{III}(X). On the other hand, both 2,4,6-trimethylpyridine and 2,4,6-trimethylpyridine·H^+ exhibited easily measured rates of catalysis for the reaction of hydrogen peroxide with (**1**)$Fe^{III}(H_2O)_2$. These results appear confusing, and further investigation with other hydroperoxides is called for in order to understand the role of general catalysis. Also, further investigations to clarify the mode of O–O bond scission [i.e., rate-determining homolytic (as in eq 1) vs heterolytic] in the reaction

$$(\mathbf{1})Fe^{III}(X) + \text{hydrogen peroxide} \xrightarrow{k_{ly}} [(\mathbf{1})(X)Fe^{IV}OH\cdot OH] \quad (1)$$

$$[(\mathbf{1})(X)Fe^{IV}OH\cdot OH] \rightarrow (\mathbf{1}^{\bullet+})(X)Fe^{IV}(O) + H_2O$$

$$[(\mathbf{1})(X)Fe^{IV}OH\cdot OH] \rightarrow (\mathbf{1})(X)Fe^{IV}OH + HO^{\bullet}$$

of hydroperoxides with iron(III) and manganese(III) porphyrins is also required. Other aspects of the past studies also require elucidation through further experimentation.

The present investigation is an extension of our previous studies and involves an examination of the reaction of *tert*-butyl hydroperoxide and cumyl hydroperoxide with (**1**)$Fe^{III}(H_2O)$ and (**1**)-Fe^{III}(OH). In this study 2,2′-azinobis(3-ethylbenzthiazoline-6-sulfonate) (ABTS) has been employed as a trap for intermediate oxidizing species. The use of ABTS is predicated on the independence of its 1e– oxidation potential on pH, its rapid 1e– oxidation, and the ability to monitor its oxidation product, $ABTS^{\bullet+}$, at a wavelength (660 nm) far removed from the iron porphyrin Soret band. The present study clarifies a number of the questions raised.

Experimental Section

All the instrumental procedures, materials, and methodologies other than those described below have been reported.[1]

Instrumentation. Isothermal GC (30 °C) was carried out on a Varian Model 3700 chromatograph equipped with a flame ionization detector coupled to a Hewlett-Packard 3392A integrator. Separation of the reaction products was achieved on a chemically bonded, fused silica capillary column (SGE, QC2/BP-1, 25 m, 0.2 mm id) using a split/splitless injector in the split mode. Propan-1-ol was used as the internal standard. HPLC analyses have been carried out with a reverse phase column (All Tech/Applied Science 250 × 4.6 mm column) packed with Lichrosorb RP-18 5μ with MeOH/H_2O (50% v/v) as the mobile phase. GC/MS measurements were carried out with a V_g 70-250 HF double focussing mass spectrometer.

Materials. Commercial ABTS (Sigma) contains a volatile impurity with the same GC retention time as $(CH_3)_2CO$. To remove this impurity ABTS was twice-dissolved in doubly distilled H_2O and concentrated to dryness under vacuum before storing in a vacuum desiccator. *tert*-Butyl hydroperoxide (9.36 M by iodometric titration[3]) was purchased from Aldrich. Cumyl hydroperoxide (Sigma, 95%) was used as received and the concentrations in solution were determined by iodometric titration.[3]

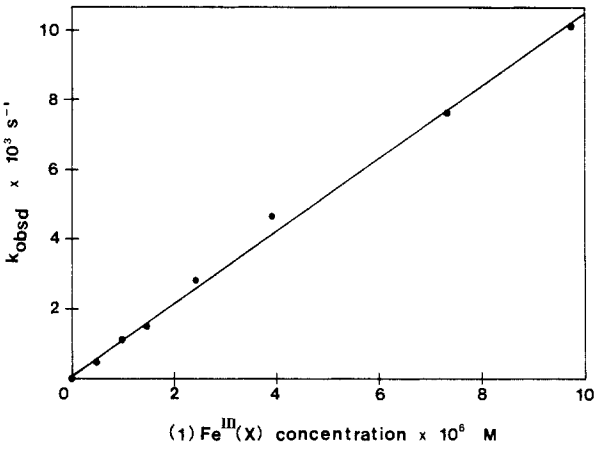

Figure 1. Dependence of pseudo-first-order rate constant for formation of $ABTS^{\bullet+}$ on concentration of (**1**)Fe^{III}(X). $[t\text{-BuOOH}]_i = 3.88 \times 10^{-5}$ and 9.75×10^{-5} M, $[ABTS]_i = 1.0 \times 10^{-2}$ M, 50 mM phosphate buffer, pH 6.87 (μ = 0.22 with $NaNO_3$) at 30 °C.

Table I. The Dependence of the Rate Constants for the Formation of $ABTS^{\bullet+}$ (k_{obsd}) on $[ABTS]_i$ at Constant $[t\text{-BuOOH}]_i$ (4.7×10^{-5} M) and pH 6.77 (NaH_2PO_4/Na_2HPO_4)

[(**1**)Fe^{III}(X)], M	$[ABTS]_i$, M	k_{obsd}, s^{-1}
1.85×10^{-6}	2.02×10^{-2}	2.18×10^{-3}
1.85×10^{-6}	1.03×10^{-2}	1.97×10^{-3}
1.85×10^{-6}	4.84×10^{-3}	1.89×10^{-3}
1.85×10^{-6}	2.02×10^{-3}	1.66×10^{-3}
4.63×10^{-6}	2.02×10^{-2}	5.66×10^{-3}
4.63×10^{-6}	1.03×10^{-2}	5.22×10^{-3}
4.63×10^{-6}	4.84×10^{-3}	4.79×10^{-3}
4.63×10^{-6}	2.02×10^{-3}	4.40×10^{-3}

Buffer solutions prepared from AnalaR sodium borate and potassium hydrogen phthalate (Mallinckrodt) were made free of heavy metal ions as described previously.[1]

The yields of products from *t*-BuOOH at the end of reaction were measured by GC analysis of aliquots (0.5 μL) of the aqueous reaction mixture. Similarly, with $Ph(CH_3)_2COOH$ the reaction was allowed to complete and 50 μL of the aqueous product solution was used for HPLC analysis.

Results

The kinetics of the reaction of *tert*-butyl hydroperoxide with (5,10,15,20-tetrakis(2,6-dimethyl-3-sulfonatophenyl)porphinato)iron(III) hydrate ((**1**)Fe^{III}(X); where X = H_2O or HO^-) have been carried out in aqueous solution (30 °C at μ = 0.22 with $NaNO_3$). The time course of the reactions was followed by use of ABTS as a 1e– oxidizable trap for the reactive oxidants produced on reaction of *t*-BuOOH with (**1**)Fe^{III}(X). These include the hypervalent iron–oxo porphyrin species and reactive oxygen radical products derived from *t*-BuOOH. It was possible, as shown in previous studies, to prevent further oxidation of $ABTS^{\bullet+}$ product to the dication, $ABTS^{2+}$, by using sufficiently high concentrations of ABTS.

The reaction system was first examined in 50 mM phosphate buffers (pH 6.30 to 6.90). It was found that ABTS is not oxidized to $ABTS^{\bullet+}$ by *t*-BuOOH in the absence of (**1**)Fe^{III}(X) nor by aerobic solutions of (**1**)Fe^{III}(X) in the absence of *t*-BuOOH; however, mixing of the three reagents rapidly generates $ABTS^{\bullet+}$. Kinetic studies were carried out in air-saturated solution under pseudo-first-order conditions with 10- to 80-fold excess *t*-BuOOH over the (**1**)Fe^{III}(X) catalyst whose concentration ranged from 4.88×10^{-7} to 9.76×10^{-6} M. The concentration of ABTS was maintained at 1.0×10^{-2} M. Under these conditions the formation of $ABTS^{\bullet+}$ follows first-order kinetics, and the pseudo-first-order rate constants (k_{obsd}) are linearly dependent on (**1**)Fe^{III}(X) catalyst concentration (Figure 1). Decreasing the large excess of ABTS

(3) Bruice, T. C.; Noar, J. B.; Ball, S. S.; Venkataram, U. V. *J. Am. Chem. Soc.* **1983**, *105*, 2452.

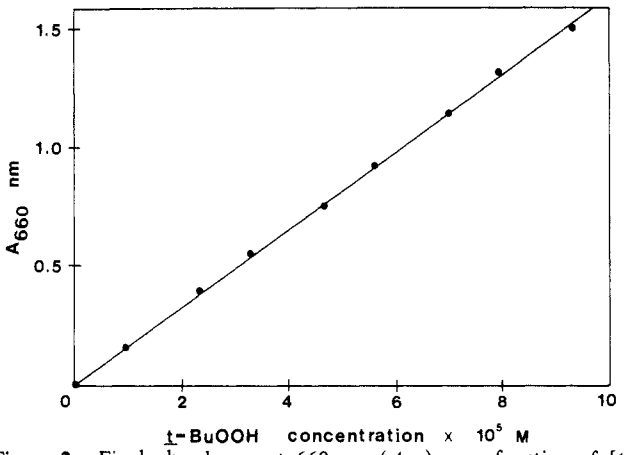

Figure 2. Final absorbance at 660 nm (A_{660}) as a function of $[t\text{-BuOOH}]_i$. $[(\mathbf{1})Fe^{III}(X)] = 9.5 \times 10^{-7}$ M, $[ABTS]_i = 4.9 \times 10^{-3}$ M, 50 mM phosphate buffer, pH 6.77 ($\mu = 0.22$ with $NaNO_3$) at 30 °C.

Table II. Dependence of k_{obsd} on $[t\text{-BuOOH}]_i$ at Constant $[(\mathbf{1})Fe^{III}(X)] = 9.5 \times 10^{-7}$ M, [ABTS] = 4.9×10^{-3} M and pH 6.77

$[t\text{-BuOOH}]_i$, M × 10^6	k_{obsd}, $s^{-1} \times 10^4$	$[t\text{-BuOOH}]_i$, M × 10^6	k_{obsd}, $s^{-1} \times 10^4$
9.36	8.71	56.2	8.38
23.4	8.60	70.2	8.65
32.7	8.62	79.6	8.77
46.8	8.52	93.6	8.40

over oxidant from 440- to 44-fold while maintaining constant $[(\mathbf{1})Fe^{III}(X)]$ (4.63×10^{-6} M) and $[t\text{-BuOOH}]$ (4.66×10^{-5} M) produces a small decrease (20%) in k_{obsd} (Table I). The above results show that the reaction is first order in $[(\mathbf{1})Fe^{III}(X)]$ and is independent of [ABTS].

A plot of the final absorbance at 660 nm vs $[t\text{-BuOOH}]_i$ reveals the linear dependence of the yield of $ABTS^{\bullet+}$ upon the latter (Figure 2). Assuming a stoichiometry of two $ABTS^{\bullet+}$ for each *t*-BuOOH consumed, the slope of the plot of Figure 2 corresponds to an oxidation yield of 68%. As expected of a process that involves the catalytic conversion of an oxidant to product under the pseudo-first-order conditions of [oxidant] ≫ [catalyst], the pseudo-first-order rate constant for product appearance is independent of [oxidant] (Table II). The initial slope obtained from plots of ΔA_{660} vs $[t\text{-BuOOH}]_i$ (Figure 3) (pH 6.77, $[(\mathbf{1})Fe^{III}(X)] = 9.5 \times 10^{-7}$ M and $[ABTS]_i = 4.9 \times 10^{-3}$ M) with a 10-fold concentration range of *t*-BuOOH is provided as an inset to Figure 3. Inspection of the inset to Figure 3 shows a linear dependence of initial rate upon the initial concentration of *t*-BuOOH oxidant with slope equal to 1.06×10^{-3} s^{-1}. When allowance is made for the 68% yield of $ABTS^{\bullet+}$ and the stoichiometry of the oxidation, this gives the first order rate constant for *t*-BuOOH consumption as 7.71×10^{-4} s^{-1}. This value compares well with the average value of $k_{obsd} = 8.58 \times 10^{-4}$ s^{-1} from first-order analysis of the rates of formation of $ABTS^{\bullet+}$. Thus, under these conditions, where the catalyst remains unsaturated in oxidant, the reaction follows the rate law of eq 2.

$$d[ABTS^{\bullet+}]/dt = k_{1y}[(\mathbf{1})Fe^{III}(X)][t\text{-BuOOH}] \quad (2)$$

$$\text{where } k_{obsd} = k_{1y}[(\mathbf{1})Fe^{III}(X)]$$

The dependence of the reaction rate on buffer concentration has been investigated with the oxygen-centered buffers: $ClCH_2COOH/ClCH_2COO^-$ (pH 3.45), CH_3COOH/CH_3COO^- (pH 4.60), $H_2PO_4^-/HPO_4^{2-}$ (pH 6.87), $H_3BO_3/H_2BO_3^-$ (pH 8.66), and HCO_3^-/CO_3^{2-} (pH 9.13). Reactions were followed at four buffer concentrations that spanned a 10-fold concentration range. Only in the case of the chloroacetic acid buffer was there any catalysis, and for this system the accelerating effect was very minor.

The dependence of k_{obsd} upon the concentration of 2,4,6-trimethylpyridine/2,4,6-trimethylpyridine·H^+ buffer at pH 6.18, 6.98, and 8.15 was investigated. At each pH there is a small inhibiting effect of this buffer on the rate of reaction. Thus, a 10-fold increase of buffer concentration (5 to 50 mM) results in approximately a 20% decrease in k_{obsd} at the three pH values investigated.

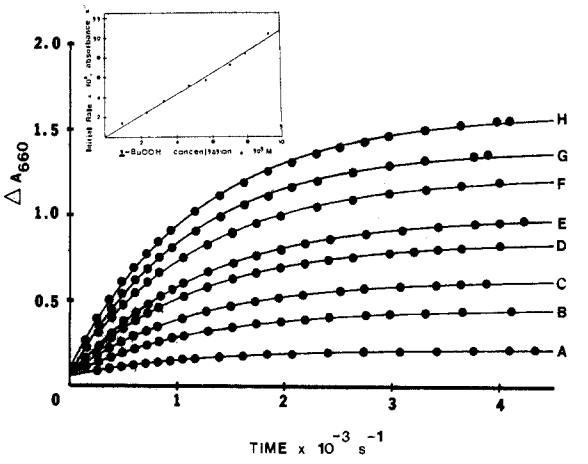

Figure 3. Change in absorbance at 660 nm, ΔA_{660}, as a function of time with different $[t\text{-BuOOH}]_i$. The points are experimental and the lines computer generated from the first-order rate law. The inset shows dependence of initial slopes, from plots of ΔA_{660} vs $[t\text{-BuOOH}]_i$, on $[t\text{-BuOOH}]_i$. $[(\mathbf{1})Fe^{III}(X)] = 9.5 \times 10^{-7}$ M, $[ABTS]_i = 4.9 \times 10^{-3}$ M, 50 mM phosphate buffer, pH 6.77 ($\mu = 0.22$ with $NaNO_3$) at 30 °C. $[t\text{-BuOOH}]_i \times 10^5$ M: (A) = 0.94; (B) = 2.34; (C) = 3.28; (D) = 4.68; (E) = 5.62; (F) = 7.02; (G) = 7.96; (H) = 9.36.

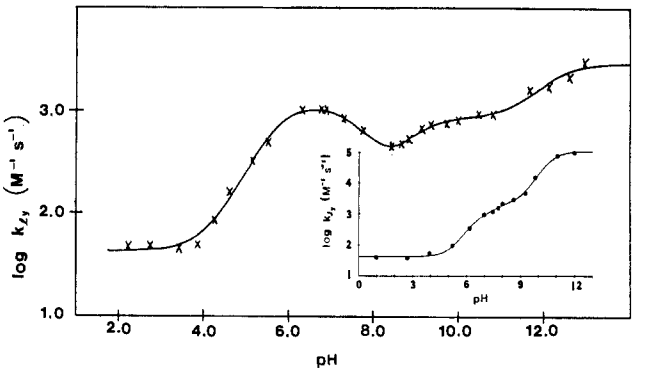

Figure 4. log values of the second-order rate constant, k_{1y}, plotted vs pH for the reaction of $(\mathbf{1})Fe^{III}(X)$ with *t*-BuOOH vs pH. $[ABTS]_i = 1.0 \times 10^{-2}$ M, $\mu = 0.22$ with $NaNO_3$, 30 °C. Inset: Computer fitting of eq 3 to a plot of log k_{1y} for the reaction of $(\mathbf{1})Fe^{III}(X)$ with H_2O_2 vs pH of ref 1.

The effect of ionic strength upon the rate of reaction of *t*-BuOOH with $(\mathbf{1})Fe^{III}(X)$ was also investigated in 10 mM phosphate buffer at pH 6.70 in the absence of $NaNO_3$ ($\mu = 0.03$). These conditions gave a second-order rate constant of 949 M^{-1} s^{-1}, and the comparable value in the presence of $NaNO_3$ ($\mu = 0.22$) is 1050 M^{-1} s^{-1}.

The pH dependence of the second-order rate constant, k_{1y}, for reaction of *t*-BuOOH with $(\mathbf{1})Fe^{III}(X)$ was determined at 26 pH values between pH 2.22 and 12.96 (Figure 4). The reactions that were carried out in solutions of pH less than 11.0 used the buffers described above. For higher pH values, the buffering by H_2O/HO^- is sufficient to maintain a constant pH. The analyses of the pseudo-first-order plots used to determine k_{1y} were complicated at pHs <5.0 and >10.0. Below pH 5.0 the formation of $ABTS^{\bullet+}$ is also brought about by O_2 and there is a slow decomposition of *t*-BuOOH presumably catalyzed by trace impurities in the system whereas above pH 10 $ABTS^{\bullet+}$ is unstable. At low pH, k_{obsd} values were obtained by analyzing the time course of the reactions with a computer program for simultaneous zero- and first-order reactions. The slope of the plot of k_{obsd} vs $[(\mathbf{1})Fe^{III}(X)]_i$ gives k_{1y}, and the non-zero intercept provides the rate constant due to adventitious oxidation. At high pH, $ABTS^{\bullet+}$ formation

Table III. Values of Rate and Equilibrium Constants Obtained from the Fitting of Equation 3 to the Experimental Points in Figure 4

k_a	43.0		
k_b	1.21×10^3		
k_c	8.57×10^2		
k_d	2.14×10^3		
K_A	2.18×10^{-6}	pK_A	5.66
K_B	2.22×10^{-8}	pK_B	7.65
K_C	1.51×10^{-9}	pK_C	8.18
K_D	1.28×10^{-12}	pK_D	12.11

Table IV. Comparison of the Second-Order Rate Constant (k_{1y}) for Reaction of *t*-BuOOH with (1)Fe^{III}(X) in the Presence and Absence of Oxygen

pH	conditions	k_{1y}, M^{-1} s^{-1}
2.50	N_2	49.6
2.72	Air	48.1
5.14	N_2	369
5.14	Air	324
6.42	N_2	930
6.32	Air	1040
10.4	N_2	960
10.4	Air	1235

is followed by its first-order disappearance. Values of k_{obsd} for $ABTS^{\bullet+}$ formation were determined by the fitting of A_{660} vs time to the rate expression for two sequential first-order reactions.

The pH dependence of the apparent second-order rate constant (k_{1y}) for reaction of (1)Fe^{III}(X) with *t*-BuOOH in the presence of ABTS is illustrated in Figure 4. The points are experimental values, and the line was generated by computer iteration from empirical eq 3. The kinetic parameters derived in this way are

$$k_{1y} = \underset{A}{\frac{k_a a_H}{(K_A + a_H)}} + \underset{B}{\frac{k_b K_A a_H}{(K_B K_A + K_A a_H + a_H^2)}} + \underset{C}{\frac{k_c K_C}{(K_C + a_H)}} + \underset{D}{\frac{k_d K_D}{(K_D + a_H)}} \quad (3)$$

given in Table III. The value of pK_D (12.1) is not known with great accuracy due to the rapid competitive destruction of $ABTS^{\bullet+}$ at the highest pH values. Thus, deletion of the value of k_{1y} at pH 12.96 provides a best fit pH vs log k_{1y} profile with $pK_D = 11.7$. Inspection of Figure 4 shows that there are four pH-independent plateaus—a bell-shaped region between pH 3.0 and 8.0 and two inflections at higher pH.

Reactions of *t*-BuOOH with (1)Fe^{III}(X) were carried out under both anaerobic and aerobic conditions in the presence of ABTS at four pH values. The results (Table IV) show that the presence of air has no effect upon k_{1y}.

The stability of (1)Fe^{III}(X) to oxidation by *t*-BuOOH in the absence of ABTS was investigated. When a solution of (1)Fe^{III}(X) (4.75×10^{-6} M; pH = 6.77) is reacted with a 10-fold excess of *t*-BuOOH in the absence of ABTS, 21% of the iron(III) porphyrin is destroyed in 30 min, and this value remains unchanged after 4 h. With an 80-fold excess of the oxidant, the loss is 44% in 4 h but it continues to a final value of 63% after 24 h. However, the data in Table I show that (1)Fe^{III}(X) is protected from oxidation in the presence of a large excess of ABTS. Thus, k_{obsd} is unaffected by the initial excess of *t*-BuOOH. Destruction of the catalyst would have led to reduced values of k_{obsd} at the higher levels of oxidant. In a separate study, the kinetics of the reaction of a solution of (1)Fe^{III}(X) = 1.9×10^{-6} M and ABTS = 9.9×10^{-3} M at pH 6.77 was examined with repeated additions of a 12-fold excess of oxidant. The k_{obsd} values from three such operations were $(1.70 \pm 0.08) \times 10^{-3}$ s^{-1}.

The products that arise from the reaction of *t*-BuOOH with (1)Fe^{III}(X) have been determined. The yield of $ABTS^{\bullet+}$ was obtained from the final values of A_{660} from the kinetic experiments, assuming that one *t*-BuOOH generates two $ABTS^{\bullet+}$ ($\epsilon_{660} = 12000$ M^{-1} cm^{-1}).[1] The yields of $ABTS^{\bullet+}$ at a given pH were independent of buffer concentration and were almost constant (ca. 70%) in the pH range 4 to 10 (Figure 5).

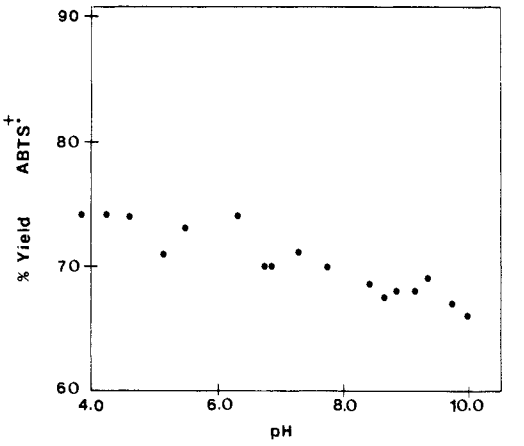

Figure 5. Variation in yield of $ABTS^{\bullet+}$ with pH in reaction of (1)-Fe^{III}(X) with *t*-BuOOH in the presence of ABTS, $\mu = 0.22$ with $NaNO_3$, 30 °C.

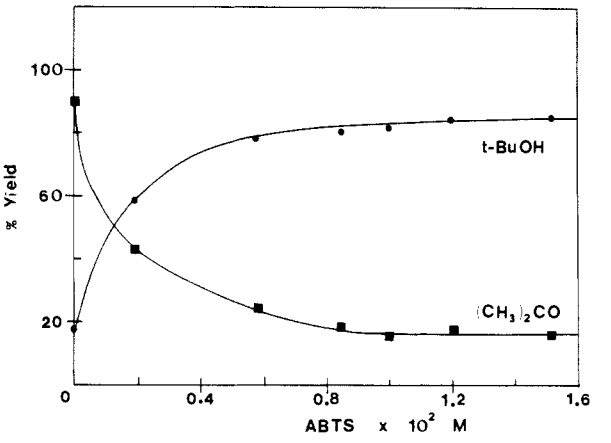

Figure 6. Dependence of percent yields of $(CH_3)_2CO$ and $(CH_3)_3COH$ on [ABTS]. [(1)Fe^{III}(X)] = 4.63×10^{-6} M, [*t*-BuOOH]$_i$ = 3.88×10^{-4} M, 50 mM phosphate buffer, pH 6.77 ($\mu = 0.22$ with $NaNO_3$) at 30 °C.

The fate of the *t*-BuOOH was examined by direct GC analysis of the reaction mixtures when all the oxidant had been consumed. The iron(III) porphyrin catalyst (4.63×10^{-6} M) was reacted with *t*-BuOOH (3.88×10^{-4} M) with a range of ABTS concentrations. The results (Figure 6) show that as the [ABTS] is increased, the *t*-BuOH yield reaches a maximum value of 84%, and that of $(CH_3)_2CO$ falls from 90% to 15%. Reactions carried out in the absence of ABTS give predominantly $(CH_3)_2CO$ while the main product from experiments with the radical trap is *t*-BuOH. The yields of $(CH_3)_2CO$ and *t*-BuOH were also examined from reactions carried out: (i) in buffered solution at six pH values between 4 and 11.5, (ii) in buffered solution (pH 6.40) in the absence of O_2, and (iii) in doubly distilled water in the absence of buffer and $NaNO_3$. These experiments employed iron(III) porphyrin at 4.75×10^{-6} M and ratios of catalyst to oxidant to ABTS of 1:80:2,100, respectively (Table V). The results show that the product distribution is independent of pH, buffer, $NaNO_3$, and O_2.

The combined yields of *t*-BuOH and $(CH_3)_2CO$ account for all the *t*-BuOOH. The carbon lost when the 4-carbon oxidant is converted to the 3-carbon $(CH_3)_2CO$ was detected as methanol. However, because the GC determination of CH_3OH in the dilute aqueous reaction solutions (less than 10^{-4} M) was erratic and unreliable, the yields of this product are not reported. To check the carbon balance, the reaction of (1)Fe^{III}(X) (1.39×10^{-5} M) with *t*-BuOOH (1.16×10^{-3} M) was carried out in triplicate in doubly distilled water in the absence of ABTS and $NaNO_3$ under argon with gas-tight capped vials. Under these conditions GC–MS analysis of the argon head space showed that neither CH_4 nor C_2H_6 was formed. For this concentration of *t*-BuOOH, GC analysis of the aqueous reaction mixture gave acetone and

Table V. Dependence of Product Yields on Reaction Conditions for the Reactions of (**1**)Fe^{III}(X) with *t*-BuOOH: [(**1**)Fe^{III}(X)] = 4.75 × 10^{-6} M, [*t*-BuOOH] = 3.88 × 10^{-4} M, and [ABTS] = 1.0 × 10^{-2} M

pH	percent yields[a] $(CH_3)_2CO$	$(CH_3)_3COH$
3.85[b]	16	79
6.40	15	81
6.40[c]	14	77
6.40[d]	12	80
8.66	16	82
10.36	17	83
11.46	14	85
e	15	84
6.77[f]	90	19
e,*f*	79	17

[a] Based on [*t*-BuOOH]$_i$. [b] Phthalate buffer was used here, since acetate buffer interferes with the GC analysis. [c] [*t*-BuOOH]$_i$ = 7.76 × 10^{-4} M. [d] Reaction carried out under anaerobic conditions. [e] Reaction in doubly distilled water in the absence of buffer and $NaNO_3$. [f] No ABTS.

methanol in 91% and 95% yields, respectively.

Five reactions, using the same concentrations of (**1**)Fe^{III}(X) and *t*-BuOOH as described above for the GC studies, were investigated in sealed reaction chambers with an O_2 electrode. Four of the reactions (pH 4.25, 6.77, 8.66, 10.36) used 50 mM buffer solutions (μ = 0.22 with $NaNO_3$) containing ABTS (1.0 × 10^{-2} M), and the fifth was carried out in doubly distilled water in the absence of ABTS and $NaNO_3$. In none of these experiments was there evidence of O_2 evolution.

Product Analysis for the reaction of cumyl hydroperoxide (9.7 × 10^{-4} M) with (1)Fe^{III}(X) (5.3 × 10^{-5} M) was carried out at four different pH values (2.19, 6.77, 10.31, and 13.0). Prior to completion of reaction, the product mixtures could not be analyzed unambiguously by GC due to the thermal decomposition of cumyl hydroperoxide in the injection port. HPLC analyses with a reverse-phase column using MeOH/H_2O (50% v/v) mixtures were carried out successfully, and the results are given in Table VI. Reactions were carried out in the presence of ABTS (7.3 × 10^{-3} M) and in its absence. When the reactions were carried out in sealed vials, with ABTS present, the $ABTS^{\bullet+}$ radical was easily observed and acetophenone was quantified by HPLC. Inspection of Table VI shows that in the presence of ABTS the maximum yield of acetophenone (34%) is obtained at pH 6.77. When there is no ABTS present, acetophenone is formed in >90% yield at pH 6.77 whereas at other pH values the yield of acetophenone is ~60 to 70%. Thus, in the absence and presence of ABTS the maximum yield of acetophenone is seen at pH 6.77.

Addition of *t*-BuOH (9.0 × 10^{-5} and 9.3 × 10^{-4} M) to the reaction of (**1**)Fe^{III}(X) (4.6 × 10^{-6} M) with *t*-BuOOH (9.0 × 10^{-5} M) has no effect upon k_{obsd} for the formation of $ABTS^{\bullet+}$ nor the yields of products.

Discussion

Several recent studies have used readily oxidized substrates as traps for the hypervalent iron-oxo porphyrin intermediate in oxygen transfer from oxidants to metallo(III) porphyrins in order to determine the rate constants for the rate-limiting oxygen-transfer step.[1,2,4] Of these studies, the very detailed investigation of the kinetics of the reaction of H_2O_2 with the non-aggregating (5,10,15,20-tetrakis(2,6-dimethyl-3-sulfonatophenyl)porphinato)iron(III) hydrate [(**1**)Fe^{III}(X), with X = H_2O and HO^-] in aqueous solution in the presence of 2,2′-azinobis(3-ethylbenzthiazoline-6-sulfonate) (ABTS) is the most relevant to the research reported here.[1] ABTS on 1e$^-$ oxidation provides the radical cation $ABTS^{\bullet+}$ which can be conveniently monitored spectrophotometrically by its absorbance at 660 nm. In the present investigation the mechanism and dynamics for the reaction of (**1**)Fe^{III}(X) with *t*-BuOOH has been studied in aqueous solution between pH 2.2 and 13.0 with trapping of reactive oxidant intermediates and products with ABTS. To understand the mechanisms and dynamics of the reaction the following observations (see Results) must be explained.

(i) At all pH values (**1**)Fe^{III}(X) catalysis of the decomposition of *t*-BuOOH is first order in both [*t*-BuOOH]$_i$ and [(**1**)Fe^{III}(X)]$_i$ (eq 2). (ii) The second-order rate constant at any pH (k_{1y}) for reaction of (**1**)Fe^{III}(X) with *t*-BuOOH is independent of [ABTS]$_i$. (iii) The reaction of *t*-BuOOH with (**1**)Fe^{III}(X) is not subjected to catalysis by oxyanion bases nor by 2,4,6-trimethylpyridine or the conjugate acids of these bases (i.e., the reaction is not subject to general-base nor general-acid catalysis at any pH). (iv) At an ABTS concentration sufficient (1 × 10^{-2} M) for maximum trapping of hypervalent iron-oxo species and *t*-BuO$^\bullet$, the products formed, at all pH values, are $ABTS^{\bullet+}$ (~70%), $(CH_3)_2C{=}O$ (15%), and *t*-BuOH (85%). Decreasing concentrations of ABTS results in a decrease in yield of *t*-BuOH and an equivalent increase in $(CH_3)_2C{=}O$. (v) Rate constants and product yields are independent of ionic strength and the presence or absence of O_2.

(vi) Whether the *tert*-butyloxo species which yields $(CH_3)_2C{=}O$ and CH_3OH is $(CH_3)_3C{-}O^\bullet$ or $(CH_3)_3C{-}O^+$ cannot be discerned from the reactions of *t*-BuOOH. However, this can be resolved by examining the products from cumyl hydroperoxide. With cumyl hydroperoxide, formation of $Ph(CH_3)_2C{-}O^+$ would result in phenyl migration and the formation of phenol (eq 4) while formation of $Ph(CH_3)_2C{-}O^\bullet$ would result in its fragmentation to acetophenone and the formation of methanol (eq 5). These results are anticipated on the basis of the greater migratory aptitude of the phenyl substituent, as a phenonium ion, when compared to methyl carbonium ion and the known facility of $CH_3^\bullet$ formation in the fragmentation of $Ph(CH_3)_2C{-}O^\bullet$.[5] It was found that acetophenone rather than phenol is the product of reaction of cumyl hydroperoxide with (**1**)Fe^{III}(X) between pH 2 and 13. Therefore, with cumyl hydroperoxide there is formed the radical intermediate $Ph(CH_3)_2C{-}O^\bullet$. It is safe to conclude that the same mechanism pertains to the reaction of *t*-BuOOH with (**1**)Fe^{III}(X). *tert*-Butoxyl radical would be the direct product of the homolytic scission of the *t*-BuO–OH bond (eq 6). It could also be formed as a product in a reaction involving heterolytic *t*-BuO–OH bond scission if the generated iron(IV)–oxo porphyrin π-cation radical were to carry out a 1e$^-$ oxidation of *t*-BuOH product (eq 7). The latter proposal is not supported by the observation that added *t*-BuOH is not oxidized in the reaction of (**1**)Fe^{III}(X) with *t*-BuOOH. It has also been shown that addition of trityl alcohol

$$Ph(CH_3)_2C{-}O^+ \rightarrow (CH_3)_2C(^+){-}O{-}Ph \rightarrow (CH_3)_2C(OH){-}O{-}Ph \rightarrow (CH_3)_2C{=}O + PhOH \quad (4)$$

$$Ph(CH_3)_2C{-}O^\bullet \rightarrow CH_3{-}CO{-}Ph + CH_3^\bullet \quad (5)$$

plausible homolytic reaction

$$(\mathbf{1})Fe^{III}(X) + t\text{-BuOOH} \rightleftarrows [(\mathbf{1})Fe^{III}(X)(t\text{-BuOOH})]$$

$$[(\mathbf{1})Fe^{III}(X)(t\text{-BuOOH})] \rightarrow (\mathbf{1})Fe^{IV}(X)(OH) + t\text{-BuO}^\bullet$$

$$t\text{-BuO}^\bullet \rightarrow (CH_3)_2C{=}O + CH_3^\bullet$$

$$(\mathbf{1})Fe^{IV}(X)(OH) + CH_3^\bullet \rightarrow (\mathbf{1})Fe^{III}(X) + CH_3OH \quad (6)$$

plausible heterolytic reaction

$$(\mathbf{1})Fe^{III}(X) + t\text{-BuOOH} \rightleftarrows [(\mathbf{1})Fe^{III}(X)(t\text{-BuOOH})]$$

$$[(\mathbf{1})Fe^{III}(X)(t\text{-BuOOH})] \rightarrow (\mathbf{1}^{\bullet+})Fe^{IV}(X)(O) + t\text{-BuOH}$$

$$(\mathbf{1}^{\bullet+})Fe^{IV}(X)(O) + t\text{-BuOH} \rightarrow (\mathbf{1})Fe^{IV}(X)(OH) + t\text{-BuO}^\bullet \quad (7)$$

(4) (a) Yuan, L.-C.; Bruice, T. C. *J. Am. Chem. Soc.* **1985**, *107*, 512. (b) Lee, W. A.; Bruice, T. C. *J. Am. Chem. Soc.* **1985**, *107*, 513. (c) Yuan, L.-C.; Bruice, T. C. *J. Am. Chem. Soc.* **1986**, *108*, 1643. (d) Lee, W. A.; Bruice, T. C. *Inorg. Chem.* **1986**, *25*, 131. (e) Balasubramanian, P. N.; Bruice, T. C. *J. Am. Chem. Soc.* **1986**, *108*, 5495. (f) Balasubramanian, P. N.; Bruice, T. C. *Proc. Natl. Acad. Sci. U.S.A.* **1987**, *84*, 1734.

(5) Meehan, E. J.; Kolthoff, I. M.; Auerbach, C.; Minato, H. *J. Am. Chem. Soc.* **1961**, *83*, 2232.

Table VI. Product Analysis for the Reaction of Cumyl Hydroperoxide (9.7×10^{-4} M) with (1)Fe^{III}(X) (5.3×10^{-5} M) at $\mu = 0.20$ ($NaNO_3$)

pH	$[ABTS]_i$, M	$[PhCOCH_3]$, M	% yield
2.19	0	6.0×10^{-4}	61.8
2.19	7.3×10^{-3}	1.1×10^{-4}	11.3
6.77	0	9.1×10^{-4}	93.8
6.77	7.3×10^{-3}	3.3×10^{-4}	34.0
10.31	0	6.9×10^{-4}	71.1
10.31	7.2×10^{-3}	2.4×10^{-4}	24.7
13.0	0	5.7×10^{-4}	59.0
13.0	7.2×10^{-3}	1.3×10^{-4}	13.4

has no effect on the yields of various products formed in the reaction of trityl hydroperoxide with (TPP)Fe^{III}(Cl) in methanol solvent.[6]

(vii) A plot of log k_{1y} vs pH (2 to 13) provides a complex profile that may be fitted by an empirical equation (eq 3) which requires four acid dissociation constants and four second-order rate constants. This is so even though each of the reactants possesses only one pK_a (i.e., t-BuOOH → t-$BuOO^-$ + H^+ and (1)$Fe^{III}(OH_2)$ → (1)Fe^{III}(OH) + H^+). What follows is a mechanistic interpretation of the reaction of t-BuOOH with (1)Fe^{III}(X) which accounts for the enumerated experimental observation—(i) through (vii).

The first-order dependence of the reaction of t-BuOOH with (1)Fe^{III}(X) on the concentrations of both reactants and the independence of rate on the concentration of the trapping agent (ABTS) shows that the rate-determining step at all pH values is the bimolecular reaction of (1)Fe^{III}(X) by t-BuOOH ((i) and (ii)). The lack of general-base and general-acid catalysis (iii), the observation of CH_3OH and $(CH_3)_2CO$ formation from t-BuOOH (iv), and the formation of CH_3–CO–Ph from cumyl hydroperoxide (vi) show that there is a homolytic breaking of the O–O bond during the course of the reaction. The initial reaction may be as shown in eq 8, followed by fragmentation of the t-BuO• to provide $(CH_3)_2CO$ plus CH_3•, etc., or homolytic O–O bond breaking may occur in a step that follows the initial reaction. The dependence of the yield of $(CH_3)_2CO$, CH_3OH, and t-BuOH upon the concentration of ABTS (Figure 6) (iv) is quantitatively accounted for by the competition of fragmentation of t-BuO• (eq 9) and trapping of both t-BuO• and (1)Fe^{IV}(X)(OH) by ABTS (eq 10). The fragmentation of t-BuO• in water has been investigated by Bors and associates,[7] who provide the first-order rate constant for the formation of $(CH_3)_2CO$ and CH_3• as 1.4×10^6 s^{-1}. These workers also report[7] the rate constant for the bimolecular reaction of ABTS with t-BuO•, in aqueous solution (2×10^9 M^{-1} s^{-1}). From the known or assumed rate constants the alternative pathways for the t-BuO• radical in water (hydrogen atom abstraction from t-BuOOH[8] and dimerization[9] (eq 11 and 12), respectively) will be unimportant. The results from the present study contrast with the very recent paper by Traylor and Xu[10] that t-BuOOH is oxidized in CH_2Cl_2 by high-valent iron–oxo species [from C_6F_5IO and (5,10,15,20-tetrakis(2,6-dichlorophenyl)porphinato)iron(III)] to give t-BuOH, $(t\text{-BuO})_2$, and O_2. The difference in the products obtained by Traylor and Xu and those from this study may arise from the different solvents used and the employment by these workers of a very electron deficient (porphyrinato)iron(III) salt. Concerning the difference in solvents, it is known that the fragmentation rate constant for t-BuO• is dramatically enhanced when the reaction is transferred from an organic solvent to water.[8] Thus, in the present study with aqueous solvent the dominant reaction of t-BuO• in the absence of ABTS is fragmentation rather than reactions (eq 11 and 12).

$$(1)Fe^{III}(X) + t\text{-BuOOH} \xrightarrow{RDS} (1)Fe^{IV}(X)(OH) + t\text{-BuO}^\bullet \quad (8)$$

$$t\text{-BuO}^\bullet \rightarrow CH_3^\bullet + (CH_3)_2CO \quad (9)$$

$$ABTS + t\text{-BuO}^\bullet + H_2O \rightarrow ABTS^{\bullet+} + t\text{-BuOH} + HO^- \quad (10)$$

$$ABTS + (1)Fe^{IV}(X)(OH) \rightarrow ABTS^{\bullet+} + (1)Fe^{III}(X)(OH)$$

$$t\text{-BuO}^\bullet + t\text{-BuOOH} \xrightarrow{k = 10^6\ M^{-1}\ s^{-1}} t\text{-BuOOH} + t\text{-BuOO}^\bullet \quad (11)$$

$$t\text{-BuO}^\bullet + t\text{-BuO}^\bullet \xrightarrow{k \sim 10^9 M^{-1}\ s^{-1}} (t\text{-BuO})_2 \quad (12)$$

Scheme I. The Nature of the Products Formed in the Commitment Steps (Included in Boxes) May Be Derived by RO–OH Bond Homolysis, as Shown Below, or May Be Derived from ROO–H Bond Homolysis (See Concluding Remarks)

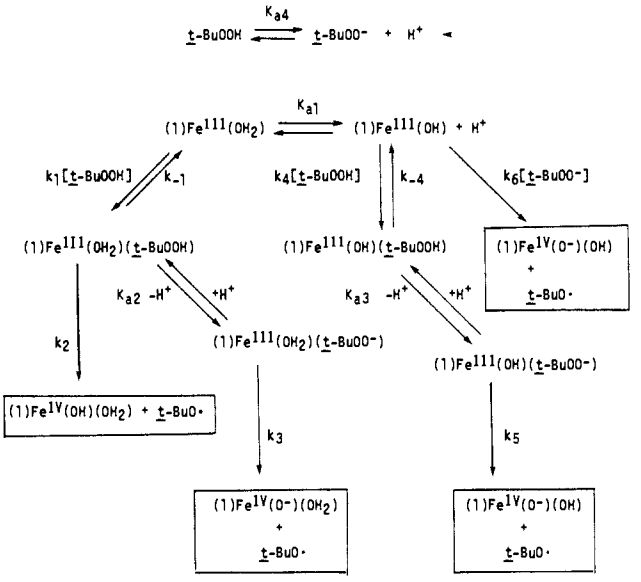

At the highest concentration of ABTS, approximately 15 to 20% of the alkoxyl radicals are found as acetone. This residual amount of acetone we attribute to fragmentation of t-BuO• within a solvent cage as shown in eq 13. This interpretation would predict that ~80% of the active intermediates escape from the solvent cage to be trapped by ABTS. The 70% yield of $ABTS^{\bullet+}$ radical is in fair agreement with this conclusion. From the rate constants given above it is unlikely, in the presence of excess ABTS, that many of the free t-BuO• fragment before they are trapped.

$$[(1)Fe^{IV}(X)(OH)\ ^\bullet OC(CH_3)_3] \xrightarrow{20\%} (1)Fe^{III}(X)(OH) + (CH_3)_2CO + CH_3OH$$

$$(1)Fe^{IV}(X)(OH) + {}^\bullet OC(CH_3)_3 \xrightarrow{H_2O,\ ABTS} (1)Fe^{III}(X)(OH) + (CH_3)_3COH + 2ABTS^{\bullet+} \quad (13)$$

The explanation for the unusual pH dependence (vii) for the reaction of t-BuOOH with (1)Fe^{III}(X) must take into account the proton dissociation of the (1)$Fe^{III}(H_2O)$ and t-BuOOH species. The sequence of reactions in Scheme I is proposed. It is not possible to fit the experimental values of the plot of log k_{1y} vs pH (Figure 4) by use of Scheme I (nor any other sequence of reactions which we could conceive) with use of preequilibrium assumptions in the complexing of the iron(III) porphyrin and *tert*-butyl hydroperoxide species. However, the steady state assumption in the four *tert*-butyl hydroperoxide–iron(III) porphyrin complexes generates an eq 14 suitable for the fitting of the log k_{1y} vs pH profile. Term A pertains to pH values <4, term B to pH 4 to 8; term C to pH 8 to 10.5, and term D to pH values >10. Since

(6) Lee, W. A.; Yuan, L.-C.; Bruice, T. C. *J. Am. Chem. Soc.* **1988**, *110*, 4277.
(7) Erben-Russ, M.; Michael, C.; Bors, W.; Saran, M. *J. Phys. Chem.* **1987**, *91*, 2362.
(8) Bors, W.; Tait, D.; Michael, C.; Saran, M.; Erben-Russ, M. *Isr. J. Chem.* **1984**, *24*, 17.
(9) Niki, E.; Kamiya, Y. *J. Am. Chem. Soc.* **1974**, *96*, 2129.
(10) Traylor, T. G.; Xu, F. *J. Am. Chem. Soc.* **1987**, *109*, 6201.
(11) Everett, A. J.; Minkoff, G. J. *Trans. Faraday Soc.* **1953**, *49*, 410.

Table VII. Values of Rate and Equilibrium Constants Derived for Equation 15 (Obtained by Comparison to Eq 3 and the Constants of Table III) for the pH Dependence of the Apparent Second-Order Rate Constants (k_{1y}) for the Reaction of *t*-BuOOH and H_2O_2 with (**1**)Fe^{III}(X) (Units are in Moles and Seconds)

equivalent kinetic terms		values of determined constants	
eq 3	eq 15	with *t*-BuOOH	with H_2O_2
k_a	$k_1k_2/(k_{-1} + k_2)$	43.0 M^{-1} s^{-1}	42.8 M^{-1} s^{-1}
k_b	k_1	1.20 × 10^3 M^{-1} s^{-1}	9.22 × 10^2 M^{-1} s^{-1}
	k_{-1}/k_2	27	20
k_c	k_4	8.57 × 10^2 M^{-1} s^{-1}	1.72 × 10^3 M^{-1} s^{-1}
k_d	k_6	2.14 × 10^3 M^{-1} s^{-1}	1.06 × 10^5 M^{-1} s^{-1}
pK_A	$p(K_{a2}k_3/k_{-1})$	5.66	6.52
pK_B	pK_{a1}	7.65	8.80
pK_C	$p(K_{a3}k_5/k_{-4})$	8.18	7.95
pK_D	pK_{a4}	12.11	10.73

pK_{a1} = 7.25[1] and pK_{a4} = 12.8,[11] eq 14 simplifies to eq 15. Comparison of eq 15 to the empirical equation (eq 3) employed to fit the experimental values of k_{1y} to the log k_{1y} vs pH profile (Figure 4) shows their mathematical equivalence.

$$k_{1y} = \underbrace{\frac{(k_2k_1)a_H^2}{(k_{-1} + k_2)(K_{a1} + a_H)(K_{a4} + a_H)}}_{A} + \underbrace{\frac{(k_3K_1K_{a2})a_H^2}{\left(\frac{k_3K_{a2}}{k_{-1}} + a_H\right)(K_{a1} + a_H)(K_{a4} + a_H)}}_{B} + \underbrace{\frac{(k_5K_{a3}K_4K_{a1})a_H}{\left(\frac{k_5K_{a3}}{k_{-4}} + a_H\right)(K_{a1} + a_H)(K_{a4} + a_H)}}_{C} + \underbrace{\frac{(k_6K_{a1}K_{a4})}{(Ka_1 + a_H)(K_{a4} + a_H)}}_{D} \quad (14)$$

$$k_{1y} = \underbrace{\frac{(k_2k_1)}{(k_{-1} + k_2)}}_{A} + \underbrace{\frac{\frac{(k_3K_{a2})k_1a_H}{(k_{-1})}}{\left(\frac{k_3K_{a2}}{k_{-1}} + a_H\right)(K_{a1} + a_H)}}_{B} + \underbrace{\frac{\frac{(k_5K_{a3})k_4}{(k_{-4})}}{\left(\frac{k_5K_{a3}}{k_{-4}} + a_H\right)}}_{C} + \underbrace{\frac{k_6K_{a4}}{(K_{a4} + a_H)}}_{D} \quad (15)$$

The constants of eq 15 were determined by comparison to the corresponding values of eq 3 provided in Table III. The constants of eq 15 have the values shown in Table VII. Inspection of Table VII shows that the kinetically apparent pK_a value for proton dissociation of (**1**)$Fe^{III}(OH_2)$ (i.e., pK_{a1}) compares favorably to the thermodynamic dissociation constant[1] (i.e., 7.65 vs 7.25). A similar favorable comparison may be made between the thermodynamic dissociation constant of *t*-BuOOH and the kinetically apparent constant pK_{a4} (12.8 vs 12.11). The enigma of the requirement of two extra kinetic dissociation constants is answered by the finding of the two-compound kinetic pK_{app} values of $p(k_3K_{a2}/k_{-1})$ and $p(k_5K_{a3}/k_{-4})$.

The constants are related to the log k_{1y} vs pH plot for *t*-BuOOH in the following manner: The rate constant at the plateau at low pH (pH 2 to 4) equals $k_1k_2/(k_{-1} + k_2)$. The rate of reaction on the ascending leg of the "Bell-shaped" portion of the plot (pH 4 to 8) is determined by $k_3K_1Ka_2/(Ka_1 + a_H)$. On the descending leg of the "Bell-shaped" plot the rate of reaction is determined by $k_3K_1Ka_2a_H/Ka_1[(k_3Ka_2/k_{-1}) + a_H]$. Thus, the rate-determining step in this pH range is k_3. By comparison of eq 3 and 15 the value of k_1 (but not k_3) can be determined. From a knowledge of $k_1k_2/(k_{-1} + k_2)$ and k_1 a value for the partition coefficient of the intermediate (**1**)$Fe^{III}(OH_2)$(*t*-BuOOH) (k_{-1}/k_2) may be calculated. The apparent acid dissociation constant which determines the ascending leg of the "Bell-shaped" curve equals k_3K_{a2}/k_{-1}. The acid dissociation constant that determines the descending leg of the "Bell-shaped" plot is K_{a1}. The rate constant provided by the second plateau (pH 8 to 10.5) equals k_4 and the apparent acid dissociation constant that determines the ascending leg to the second plateau is equal to k_5K_{a3}/k_{-4}. In this pH range the rate of reaction is given by $k_5K_4Ka_3/[(k_5Ka_3/k_{-4}) + a_H]$ so that k_5 is part of the kinetically apparent pK_C term and when $a_H > (k_5K_{a3}/k_{-4})$ k_5 is rate determining. The values of k_3 and k_5 cannot be determined independently. Finally, the plateau at high pH (pH >10.5) is generated from the rate constant k_6 and acid dissociation constant K_{a4}.

Comparison of the Various Kinetic Parameters Obtained for the Reaction of (1)Fe^{III}(X) with Hydrogen Peroxide and *tert*-Butyl Hydroperoxide. The log k_{1y} vs pH profile for the reaction of (**1**)Fe^{III}(X) with H_2O_2 has been published.[1] Like the profile for *t*-BuOOH, the profile for H_2O_2 (inset to Figure 4) may be favorably fit by eq 3 and 15. The constants obtained by doing so are included in Table VII. It was originally proposed[1] with H_2O_2 that the kinetically apparent acid dissociation responsible for increase in log k_{1y} in the acid pH range was that for (**1**)$Fe^{III}(OH_2)$ → (**1**)$Fe^{III}(OH)$ + H^+. That pK_{a1} (Scheme I) exceeded the kinetically apparent pK_a (pK_{app}) by 0.7 was explained by the assumption of a preequilibrium prior to the rate-limiting step.[1] It is noted that with *t*-BuOOH the value of pK_{a1} exceeds pK_{app} by 1.6. This K_{app} is now suggested to be associated with K_{a2} which is the ionization constant of the hydroperoxide after it is ligated to (**1**)$Fe^{III}(H_2O)$. The constant K_{a2} is obtained only as part of the compound term ($K_{a2}(k_3/k_{-1})$) where k_3/k_{-1} is the partitioning coefficient of the steady state intermediates (**1**)$Fe^{III}(OH_2)$(*t*-BuOOH) + (**1**)$Fe^{III}(OH_2)$(*t*-$BuOO^-$). The increase in log k_{1y} with increase in pH from 8 to 10 for *t*-BuOOH leading to a plateau region in the pH profile is also associated with a pK_{app} that derives from the acid dissociation of ligated hydroperoxide [i.e., (**1**)-Fe^{III}(OH)(*t*-BuOOH) → (**1**)Fe^{III}(OH)(*t*-$BuOO^-$) + H^+]. Again, the kinetic pK_{app} equals the product of the true pK_a and the partitioning of ligated species [i.e., $p(K_{a3}(k_5/k_{-4})]$.

The following comparisons of the derivable rate constants for *t*-BuOOH and H_2O_2 can be made from the data of Table VII. The value of the rate constant for the first plateau ($k_1k_2/(k_{-1} + k_2)$) at low pH is seen to be the same for both hydroperoxides. The partitioning coefficient for the intermediate (k_{-1}/k_2) is also much the same. This shows that in acidic solution neither steric nor polar effects of the hydroperoxides have much influence on the rate. Such a finding is in accord with a previous investigation of the reactions of a number of hydroperoxides with (5,10,15,20-*meso*-tetraphenylporphinato)iron(III) chloride ((TPP)Fe^{III}(Cl)) in CH_3OH.[4b,6] The lack of importance of steric effects is also seen in the reaction of hydroperoxides with (TPP)Cr^{III}(Cl),[4a] (TPP)Mn^{III}(ImH)(Cl),[4c] and (TPP)Co^{III}(Cl)[4d] in organic solvents. The unimportance of steric and polar effects, for reactions of hydroperoxides, is also seen in the favorable comparison of the values of the rate constant for ligation of undissociated hydroperoxides to (**1**)$Fe^{III}(OH_2)$ and (**1**)Fe^{III}(OH). Thus, k_1 for *t*-BuOOH and H_2O_2 are essentially identical and k_4 for *t*-BuOOH and H_2O_2 differ by only a factor 2. However, the rate constant (k_6) for reaction of HO_2^- with (**1**)Fe^{III}(OH) exceeds that for the reaction with *t*-$BuOO^-$ by 70-fold. This may reflect a more favorable ligation with HO_2^- or a greater reactivity of the ligated HO_2^- species. One may conclude that although the shapes of the log k_{1y} vs pH profiles for *t*-BuOOH and H_2O_2 differ somewhat (at a maximum of only 0.4 kcal·M^{-1}) the associated rate constants are much the same below pH 10. Studies with other alkyl hydroperoxides are required.

Concluding Remarks

The products formed when cumyl hydroperoxide and its anion react with (**1**)$Fe^{III}(OH_2)$ and (**1**)Fe^{III}(OH) are acetophenone and

Scheme II. Units for Rate Constants Are Moles and Seconds

$(1)Fe^{III}(X) + t\text{-BuOOH} \rightarrow [(1)(X)Fe^{IV}(OH)\,{}^{\bullet}O\text{-}C(CH_3)_3]$	$k_a\ 10^3$	(A)
$[(1)(X)Fe^{IV}(OH)\,{}^{\bullet}O\text{-}C(CH_3)_3] \rightarrow (1)(X)Fe^{IV}OH + (CH_3)_3CO^{\bullet}$	$k_b > 1.2$	(B)
$[(1)(X)Fe^{IV}OH\,{}^{\bullet}O\text{-}C(CH_3)_3] \rightarrow (1)(X)Fe^{III} + CH_3OH + (CH_3)_2C{=}O$	$k_c > 9 \times 10^{-2}$	(C)
$(1)(X)Fe^{IV}OH + ABTS \rightarrow (1)Fe^{III}(X) + ABTS^{\bullet+}$	$k_d > 50$	(D)
$(CH_3)_3CO^{\bullet} + ABTS \rightarrow (CH_3)_3COH + ABTS^{\bullet+}$	$k_e\ 1 \times 10^9$	(E)
$(CH_3)_3CO^{\bullet} \rightarrow (CH_3)_2C{=}O + CH_3^{\bullet}$	$k_f\ 1 \times 10^6$	(F)
$CH_3^{\bullet} + (1)(X)Fe^{IV}OH \rightarrow CH_3OH + (1)Fe^{III}(X)$	$k_g > 1 \times 10^6$	(G)

methanol. Acetophenone is the expected fragmentation product of $Ph(CH_3)_2C\text{-}O^{\bullet}$. The latter would be the direct product of the homolytic cleavage of cumyl hydroperoxide. General catalysis cannot be detected at any pH in the reactions involving *t*-BuOOH. (A complete kinetic study with $Ph(CH_3)_2COOH$ is in progress.) According to Traylor and co-workers[12] general-base catalysis is an expectation for heterolytic RO–OH bond breaking in the reaction of ROOH species with iron(III) porphyrins. In addition, the lack of sensitivity of the second-order rate constant for reaction of $(TPP)Fe^{III}(Cl)$ with hydroperoxides (YOOH) to the pK_a of YOH in both methanol[4b,6] and similar observation with $(1)Fe^{III}(X)$ at pH 6.7 in water[13] is strongly suggestive of a homolytic reaction. Details of the mechanism may well be pH dependent as is k_{1y}. For simplicity, only two kinetically competent mechanisms will be considered.

The first involves homolysis of the hydroperoxide O–O bond in the rate-determining step and is shown in Scheme II (where [ ] indicates solvent caged species). The rate constants of Scheme II, obtained by computer simulation, pertain to pH 6.77. Scheme II is in accord with (i) the bimolecular reaction of *t*-BuOOH with $(1)Fe^{III}(X)$ being rate limiting, (iv) acetone and methanol being obtained in 15% yield at saturating concentrations of ABTS, and (vi) the reaction being homolytic. Both k_e for the trapping of $(CH_3)_3C\text{-}O^{\bullet}$ by ABTS in aqueous solution and k_f for the fragmentation of $(CH_3)_3C\text{-}O^{\bullet}$ in aqueous solution are from literature sources.[7,8] The constant k_a is rate determining and equals k_{1y} at pH 6.77. The constants k_b, k_c, k_d, and k_g are given as the minimal numbers that are kinetically competent. By trapping of uncaged $(1)Fe^{IV}(X)(OH)$ and $^{\bullet}O\text{-}C(CH_3)_3$ by ABTS 2 equiv of $ABTS^{\bullet+}$ are formed per equivalent of *t*-BuOOH, plus *t*-BuOH and $(1)Fe^{III}(X)$. In the absence of ABTS the products of *t*-BuOOH are predominantly CH_3OH and $(CH_3)_2C{=}O$.

A second homolytic mechanism is shown in Scheme III.

Scheme III

$$(1)Fe^{III}(X) + (CH_3)_3COOH \rightarrow [(1)(X)Fe^{IV}(OH)\,{}^{\bullet}O\text{-}C(CH_3)_3] \quad (H)$$

$$[(1)(X)Fe^{IV}(OH)\,{}^{\bullet}O\text{-}C(CH_3)_3] \rightarrow (1)Fe^{III}(X) + (CH_3)_2CO + CH_3OH \quad (I)$$

$$(1)Fe^{III}(X) + (CH_3)_3COOH \rightarrow (1)Fe^{II}(X) + (CH_3)_3CO_2^{\bullet} + H^+ \quad (J)$$

$$2(CH_3)_3CO_2^{\bullet} \rightarrow 2(CH_3)_3CO^{\bullet} + O_2 \quad (K)$$

$$(1)Fe^{II}(X) + O_2 \rightarrow (1)Fe^{III}(X)O_2 \quad (L)$$

$$(1)Fe^{II}(X) + (1)Fe^{III}(X)O_2 \rightarrow (1)(X)Fe^{III}O\text{–}OFe^{III}(X)(1) \quad (M)$$

$$(1)(X)Fe^{III}O\text{–}OFe^{III}(X)(1) \rightarrow 2(1)Fe^{IV}(X)(O) \quad (N)$$

$$(CH_3)_3CO^{\bullet} \rightarrow CH_3^{\bullet} + (CH_3)_2C{=}O \quad (O)$$

$$(1)Fe^{IV}(X)(O) + CH_3^{\bullet} \rightarrow (1)Fe^{III}(X) + CH_3OH \quad (P)$$

Reactions H and I are the same as A and C in Scheme II and account for the 15% cage oxidation to provide CH_3OH and $(CH_3)_2C{=}O$. In competition with this process is the reduction of the iron(III) porphyrin species by hydroperoxide, reaction J, and following reactions that involve molecular oxygen. Partially rate determining would be steps H and J. The reactions of eq L, M, and N have been reported by Balch and associates.[14] Summation of the reactions J to P provides eq 16. Thus, reactions J to P provide the same products as do reactions H and J and the

$$(CH_3)_3COOH \xrightarrow{(1)Fe^{III}(X)} (CH_3)_2C{=}O + CH_3OH \quad (16)$$

reactions of Scheme II. For Scheme III to be valid it must be assumed that ABTS acts only as a trap for the uncaged species $(1)Fe^{IV}(X)(O)$ (reaction N) and $(CH_3)_3CO^{\bullet}$ (reaction K). If ABTS traps $(CH_3)_3C\text{–}OO^{\bullet}$ the reactions of Scheme IV would be competent in the presence of ABTS. Aside from reactions H and I, such a process would amount to simple Fenton chemistry.

Scheme IV

$$(1)Fe^{III}(X) + (CH_3)_3COOH \rightarrow [(1)(X)Fe^{IV}(OH)\,{}^{\bullet}O\text{-}C(CH_3)_3] \quad (H)$$

$$[(1)(X)Fe^{IV}(OH)\,{}^{\bullet}O\text{-}C(CH_3)_3] \rightarrow (1)Fe^{III}(X) + (CH_3)_2CO + CH_3OH \quad (I)$$

$$(1)Fe^{III}(X) + (CH_3)_3COOH \rightarrow (1)Fe^{II}(X) + (CH_3)_3COO^{\bullet} + H^+ \quad (J)$$

$$(CH_3)_3COO^{\bullet} + ABTS + H_2O \rightarrow (CH_3)_3COOH + ABTS^{\bullet+} + HO^- \quad (Q)$$

$$(1)Fe^{II}(X) + (CH_3)_3COOH \rightarrow (1)Fe^{III}(X)(OH) + (CH_3)_3CO^{\bullet} \quad (R)$$

$$(CH_3)_3CO^{\bullet} + ABTS + H_2O \rightarrow (CH_3)_3COH + ABTS^{\bullet+} + HO^- \quad (S)$$

Replacement of reactions H and I of Scheme IV by reactions T and U would provide a competent mechanism which involves only Fenton chemistry. One may note that $CH_3^{\bullet}$ has been reported[15] to react with iron(III) porphyrins to product CH_3OH ($k = 2.3 \times 10^9\ M^{-1}\ s^{-1}$ in 1/1 (v/v) H_2O:2-propanol solvent). Evidence is now being sought to differentiate these mechanisms for the reactions that occur in the four distinct regions of the log k_{1y} vs pH profile.

$$(1)Fe^{II}(X) + (CH_3)_3CO_2H \rightarrow [(1)(X)Fe^{III}(OH)\,{}^{\bullet}O\text{-}C(CH_3)_3] \quad (T)$$

$$[(1)(X)Fe^{III}(OH)\,{}^{\bullet}O\text{-}C(CH_3)_3] \rightarrow (1)Fe^{II}(X) + (CH_3)_2CO + CH_3OH \quad (U)$$

Acknowledgment. This work was supported by the National Institutes of Health and the National Science Foundation. J. R.L.S. thanks the SERC (UK) for travel funds to visit and carry out research at the University of California, Santa Barbara.

(12) Traylor, T. G.; Lee, W. A.; Stynes, D. V. *J. Am. Chem. Soc.* **1984**, *106*, 755.
(13) Balasubramanian, P. N.; Lee, R. W.; Bruice, T. C., unpublished results.
(14) Balch, A. L.; Chan, Y. W.; Cheng, R. J.; La Mar, G. N.; Latos-grazynski, L.; Renner, M. W. *J. Am. Chem. Soc.* **1984**, *106*, 7779.
(15) Brault, D.; Neta, P. *J. Am. Chem. Soc.* **1981**, *103*, 2705.